Supramolecular Chemistry

DOI: 10.1002/ange.201310571

Hydrophobic Self-Assembly Affords Robust Noncovalent Polymer Isomers**

*Jonathan Baram, Haim Weissman, Yaron Tidhar, Iddo Pinkas, and Boris Rybtchinski**

In memory of Michael Bendikov

Abstract: *In covalent polymerization, a single monomer can result in different polymer structures due to positional, geometric, or stereoisomerism. We demonstrate that strong hydrophobic interactions result in stable noncovalent polymer isomers that are based on the same covalent unit (amphiphilic perylene diimide). These isomers have different structures and electronic/photonic properties, and are stable in water, even upon prolonged heating at 100°C. Such combination of covalent-like stability together with structural/functional variation is unique for noncovalent polymers, substantially advancing their potential as functional materials.*

Strong covalent bonds enable the connection of identical reactive molecular units in diverse ways, thus resulting in stable isomers which often have different chemical and physical properties. Polymerization is the most prominent example of such variable connectivity, where a single monomer can result in different polymer structures as a result of positional, geometric, or stereoisomerism, which is utilized to control polymer properties. In contrast, noncovalent polymerization is usually based on weaker bonding, which is inadequate to produce polymer isomers that do not interconvert. In fact, most noncovalent polymers are designed as reversible systems so as to form a single thermodynamic product capable of self-repair and facile depolymerization.[1] Nevertheless, there is growing recent interest in robust noncovalent polymeric materials,[1a,2] and strategies aimed at their rational design.[3] In this respect, the concept of robust supramolecular polymer isomers having different structure and function would broaden the scope of noncovalent polymerization. Hydrophobic interactions appear to be the most suitable to emulate covalent polymerization as they can be sufficiently strong to dramatically influence chemical properties,[4] and create robust functional materials from well-defined amphiphiles.[5] While the hydrophobic assemblies are robust in neat water, the presence of an organic solvent mitigates hydrophobic bonding to render the assemblies dynamic and adaptive.[6]

Herein we report on the employment of a single building block to assemble two supramolecular polymer isomers in water, two isomers that have different structures as well as electronic and photophysical properties. These polymers are remarkably stable in neat aqueous solutions, but can be interconverted using organic solvents.

The primary building block, the amphiphilic perylene diimide (PDI) compound **1**, was designed to have an extended

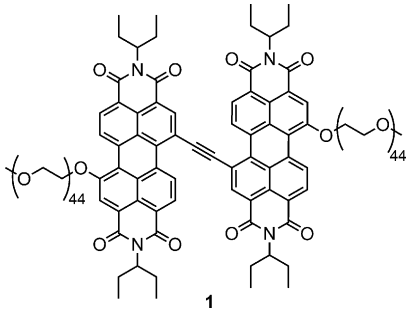

1

flat aromatic core to provide strong hydrophobic interactions, and long PEG chains (PEG44) to render it soluble in neat water (see the Supporting Information). The analogue of **1** having shorter PEG chains (PEG17) is not soluble in water, and shows self-assembly behavior (in water/THF mixtures) different from that of **1**.[7]

The compound **1** is readily dissolved in water to form a green solution (the green-colored assemblies are designated as **1G**, and can be converted into the purple-brown assemblies **1P**; see below). UV/vis spectra of **1G** exhibit significant red shifts and absorption-band broadening in comparison to disaggregated **1** (Figure 1). Imaging by cryo-TEM reveals the formation of fibrous structures which are (2.1 ± 0.3) nm in width and tens of nanometers in length (Figure 2A). The assemblies are stable in water solutions at ambient conditions, and remain unchanged for at least 21 months (see Figure S5 in

[*] Dr. J. Baram, Dr. H. Weissman, Dr. Y. Tidhar, Prof. B. Rybtchinski
Department of Organic Chemistry, Weizmann Institute of Science, Rehovot 76100 (Israel)
E-mail: boris.rybtchinski@weizmann.ac.il
Homepage: http://www.weizmann.ac.il/oc/boris/
Dr. I. Pinkas
Department of Chemical Research Support, Weizmann Institute of Science (Israel)

[**] This work was supported by grants from the Israel Science Foundation, Minerva Foundation, Schmidt Minerva Center for Supramolecular Architectures, and the Helen and Martin Kimmel Center for Molecular Design. The EM studies were conducted at the Irving and Cherna Moskowitz Center for Nano and Bio-Nano Imaging (Weizmann Institute). Transient absorption studies were performed at the Dr. J. Trachtenberg laboratory for photobiology and photobiotechnology (Weizmann Institute). We thank Dr. Elisha Krieg for valuable discussions and Drs. Raanan Carmieli and Lev Weiner for their help with EPR studies. I.P. acknowledges support by a research grant from the Leona M. and Harry B. Helmsley Charitable Trust.

Supporting information for this article is available on the WWW under http://dx.doi.org/10.1002/anie.201310571.

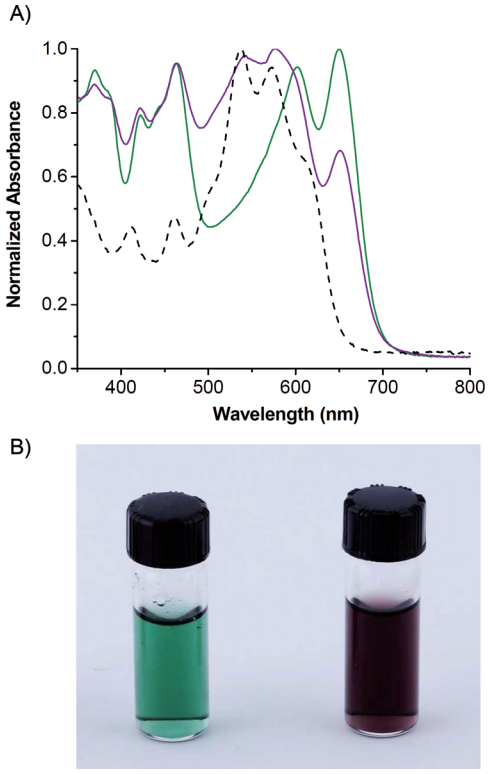

Figure 1. A) Normalized UV/vis spectra of 1×10^{-5} M solutions of **1** in THF (dashed line), **1G** in water (green line), and **1P** in water (purple line). B) Photograph of water solutions (1×10^{-5} M) of **1G** (left) and **1P** (right).

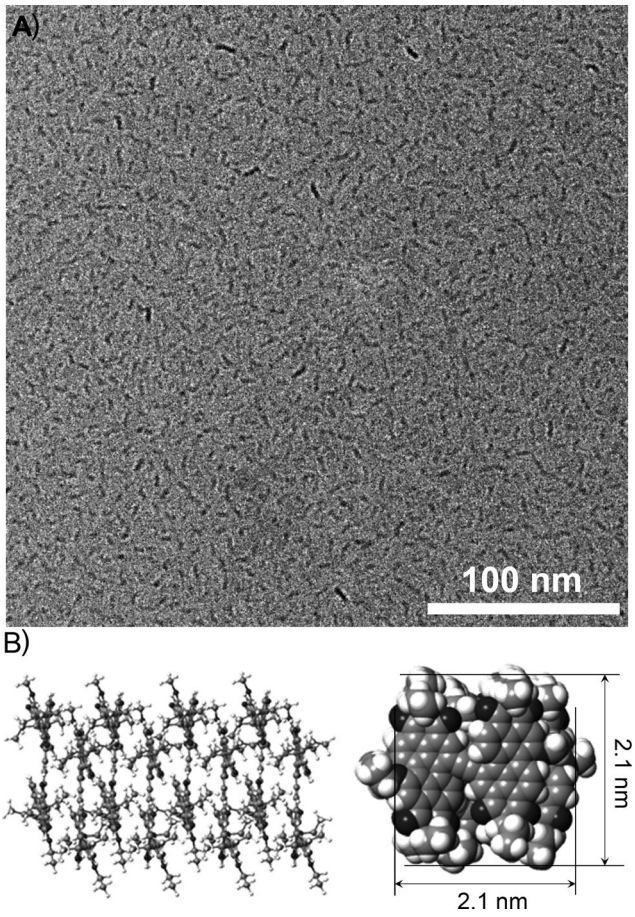

Figure 2. A) Cryo-TEM image of **1G** in water (1×10^{-4} M). B) Molecular model. Side view (space-filling representation on right) corresponds to the fiber cross-section.

the Supporting Information). The molecular model that fits best the fiber dimensions is a one-dimensional molecular stack of **1**, with an alternating ladder arrangement of the PDI cores (Figure 2B), featuring both longitudinal and transverse shifts between the PDIs. This interaction mode is consistent with the observed red shifts and broadening in the UV/vis spectra.[8]

When **1** is assembled in water/THF solutions, a more complex sequence of self-assembly events is observed. Upon adding a THF solution of **1** to water (10^{-5}–10^{-4} M, THF content 20–40 vol%), an immediate color change from dark purple to green occurs. Cryo-TEM revealed that the green assembly product has a fibrous morphology (see Figure S7 in the Supporting Information), similar to that of **1G** (obtained upon dissolving **1** in neat water). After the initial formation of the green nanofibers, a color change from green to purple-brown is observed (within 1.5 h at 40% THF content and 10^{-4} M concentration of **1**). When the process is completed, THF is evaporated and water is added to result in a 10^{-4} M purple-brown solution (**1P**, Figure 1B); these are conditions identical to the ones under which **1G** was obtained. Cryo-TEM imaging reveals formation of long aligned fibers having a (1.8 ± 0.2) nm width and covering the entire imaged area, thus implying fiber lengths of at least ten microns (Figure 3A and Figure S10 in the Supporting Information). The interfiber spacing is (4.4 ± 0.7) nm (lighter contrast areas), which corresponds to partially folded PEG chains.[9] The fiber width and interfiber distances are in good agreement with the center-to-center spacing of 6.2 nm revealed by FFT (Figure 3A). Rheological measurements indicate a low degree of interaction between the fibers (see Figure S11 in the Supporting Information), despite their alignment observed in cryo-TEM. Gradual formation of **1P** is also observed upon addition of THF to a solution of **1G** in neat water. Thus, in agreement with our previous work,[6] THF attenuates hydrophobic interactions to allow rearrangement of molecular building blocks, thereby resulting in the transformation of kinetically trapped hydrophobic assemblies into more stable ones (**1G**→**1P**). The molecular model of **1P** that fits best the cryo-TEM data is a stack motif with the uniform transverse shift pattern and tighter molecular packing in comparison to that of **1G** (Figure 2B). Importantly, **1P** and **1G** display different interaction modes between the aromatic cores as evidenced by UV/vis and cryo-TEM, with higher overlap and face-to-face stacking (*H*-aggregation) in the case of **1P**, whereas in **1G**, a *J*-aggregation (slipped stack) motif is also present.

In addition to being stable for months at ambient conditions, nanofibers of **1G** and **1P** are also remarkably stable towards heating in water solutions. Upon heating of either **1G** or **1P** at 100 °C for 24 hours, the assemblies' structures are unaffected as evidenced by UV/vis and cryo-

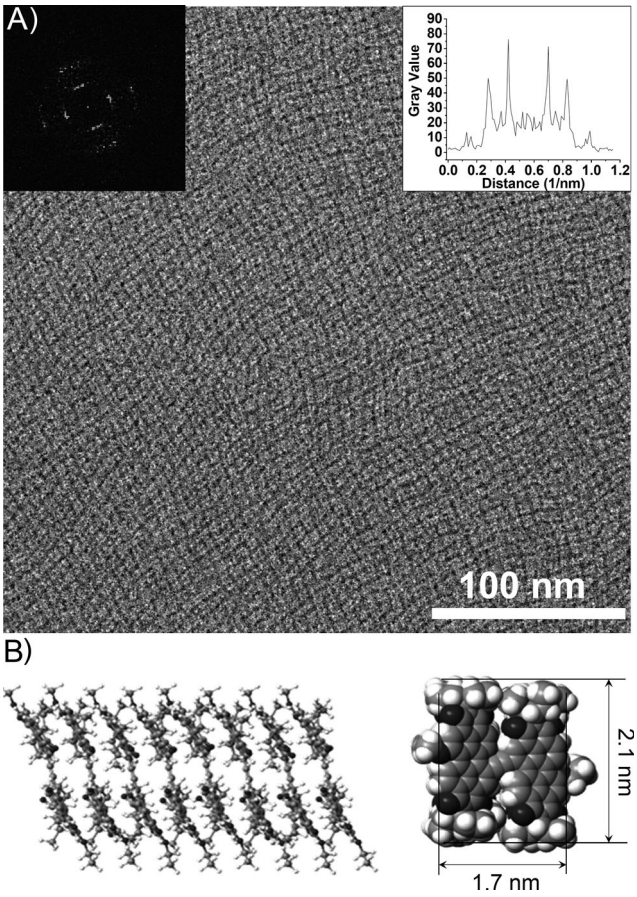

Figure 3. A) Cryo-TEM image of **1P** in water (1×10^{-4} M). Insets: FFT (left) and the corresponding distance profile (left). B) Molecular model. Side view (space-filling representation on right) corresponds to the fiber cross-section.

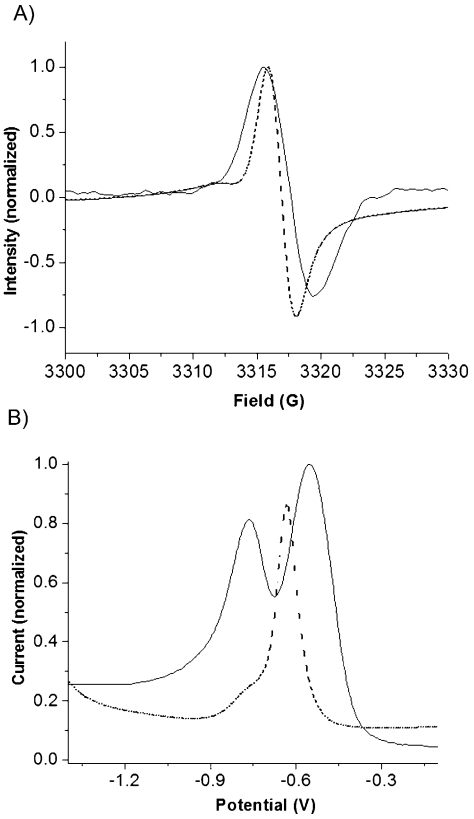

Figure 4. Spectra (normalized) of **1G** (solid line) and **1P** (dash line) in water. A) Electron paramagnetic resonance (EPR) spectra; reduction with sodium dithionite. B) Differential pulse voltammetry (dPV).

TEM (see Figures S6, S8, and S10 in the Supporting Information). The lack of transformation upon heating indicates a high kinetic barrier ($\geq$35 kcal mol^{-1}). Such stability is unique for noncovalent polymers. Notably, drying of either **1G** or **1P** from aqueous solutions and redissolving in neat water does not result in appreciable change in the UV/vis spectra. Although highly stable in water and having the ability to retain the structural motifs upon drying, the assemblies can be interconverted using organic solvents. Thus, **1G** can be converted into **1P** by addition of THF (see above), and the reverse, **1P**→**1G** transformation, is achieved by dissolving **1P** (dried from water) in chloroform or THF with subsequent solvent evaporation and re-dissolution in water. The mechanism of the **1G**→**1P** transformation in water/THF solutions, and the factors leading to the kinetically favored formation of **1G** are currently under study.

A mixture of aqueous **1G** and **1P** (1:1 ratio) gives rise to a UV/vis spectrum that is a sum of individual spectra (see Figure S4 in the Supporting Information). It remains unchanged over several weeks at room temperature and upon heating to 100 °C for 24 hours, indicating that the two assemblies coexist without interconversion, further confirming their high stability in water.

Electrochemical studies by cyclic voltammetry (CV) and differential pulse voltammetry (DPV) of disaggregated **1** (dichloromethane solution; see Figures S3 and S9 in the Supporting Information) reveal four one-electron reductions (−0.7, −0.76, −1.02, and −1.5 V vs. SCE), as expected for the accommodation of two electrons by each PDI unit.[7] Remarkably, **1G** and **1P** demonstrate dissimilar potentiodynamic characteristics. The CV and DPV of **1G** display two redox potentials at −0.78 and −0.57 V vs. SCE, and appear as broad peaks in DPV, whereas **1P** exhibits a very different pattern—a sharp peak at −0.62 V vs SCE (Figure 4B). Thus, the electrochemistry is strongly influenced by the aggregation modes.[10] The sharp peak in the case of **1P** is consistent with uniform structure and stronger electronic coupling resulting from extensive overlap of the aromatic moieties. Two distinct reduction peaks for **1G** point to a lesser degree of coupling and greater similarity to the individual molecules of **1**.

To further characterize the electronic properties of **1P** and **1G**, we performed partial reduction experiments to create PDI radical anions embedded within the aromatic stacks. The radical anions give rise to an EPR signal (Figure 4A), whose width depends on a number of stacked PDIs involved in electron hopping.[11] Following reduction using sub-equivalent amounts of sodium dithionite, the EPR spectrum of partially reduced **1P** exhibits a peak having a width of 2.2 G, which is consistent with electron hopping over three molecules. However, the EPR signal of partially

reduced **1G** has a width of 3.8 G, which is almost identical to the width observed for partially reduced **1** in THF, indicating that there is no significant intermolecular electron hopping in **1G** (Figure 4A and Figure S9). Stronger electronic communication between the molecular units in **1P** is consistent with the electrochemical data, further underscoring differences in electronic properties of **1P** and **1G**.

Femtosecond transient absorption studies were carried out to probe the excited state dynamics of **1G** and **1P**. Laser-power dependence of the excited state decay reveals dissimilar exciton annihilation[9] behavior for **1P** and **1G** (see Figure S12 in the Supporting Information). The **1G** nanofibers exhibit a superior exciton hopping as evidenced by stronger power dependence, and may be attributed to the contribution of the *J*-aggregation mode and longer exciton lifetimes in **1G**, thus favoring efficient exciton hopping.[12]

Distinct electronic and photonic properties of **1G** and **1P** arise from different patterns of π–π interactions. Greater overlap of the aromatic cores in **1P** brings about stronger electronic coupling and more efficient electron delocalization. In contrast, the **1G** structure favors efficient exciton hopping. Thus, self-assembly of **1** can be driven towards remarkably stable arrays having either electron- or exciton-transfer propensities. Such convenient tuning of function can facilitate fabrication of photonic and electronic materials with predesigned properties.

In conclusion, strong hydrophobic interactions enable the assembly of two robust noncovalent polymer isomers from a single building block. The polymers exhibit different structure and function under identical conditions and do not interconvert in water, even upon prolonged heating. Such a combination of stability and functional diversity is unique for noncovalent polymers. Noncovalent polymerization, leading to stable polymer isomers with different function, emulates its covalent counterpart, and may advance the applicability of noncovalent materials.

Received: December 5, 2013
Published online: March 18, 2014

Keywords: hydrophobic effect · isomers · noncovalent interactions · self-assembly · supramolecular chemistry

[1] a) T. Aida, E. W. Meijer, S. I. Stupp, *Science* **2012**, *335*, 813–8177; b) L. Brunsveld, B. J. B. Folmer, E. W. Meijer, R. P. Sijbesma, *Chem. Rev.* **2001**, *101*, 4071–4097; c) R. P. Sijbesma, F. H. Beijer, L. Brunsveld, B. J. B. Folmer, J. H. K. K. Hirschberg, R. F. M. Lange, J. K. L. Lowe, E. W. Meijer, *Science* **1997**, *278*, 1601–1604; d) S. C. Zimmerman, F. Zeng, D. E. C. Reichert, S. V. Kolotuchin, *Science* **1996**, *271*, 1095–1098.

[2] a) B. Rybtchinski, *ACS Nano* **2011**, *5*, 6791–6818; b) D. Görl, X. Zhang, F. Würthner, *Angew. Chem.* **2012**, *124*, 6434–6455; *Angew. Chem. Int. Ed.* **2012**, *51*, 6328–6348; c) T. Fenske, H.-G. Korth, A. Mohr, C. Schmuck, *Chem. Eur. J.* **2012**, *18*, 738–755.

[3] a) M. Bellot, L. Bouteiller, *Langmuir* **2008**, *24*, 14176–14182; b) F. Fennel, S. Wolter, Z. Q. Xie, P. A. Plotz, O. Kuhn, F. Würthner, S. Lochbrunner, *J. Am. Chem. Soc.* **2013**, *135*, 18722–18725; c) P. A. Korevaar, S. J. George, A. J. Markvoort, M. M. J. Smulders, P. A. J. Hilbers, A. P. H. J. Schenning, T. F. A. De Greef, E. W. Meijer, *Nature* **2012**, *481*, 492–496.

[4] P. Mal, B. Breiner, K. Rissanen, J. R. Nitschke, *Science* **2009**, *324*, 1697–1699.

[5] E. Krieg, H. Weissman, E. Shirman, E. Shimoni, B. Rybtchinski, *Nat. Nanotechnol.* **2011**, *6*, 141–146.

[6] Y. Tidhar, H. Weissman, S. G. Wolf, A. Gulino, B. Rybtchinski, *Chem. Eur. J.* **2011**, *17*, 6068–6075.

[7] J. Baram, E. Shirman, N. Ben-Shitrit, A. Ustinov, H. Weissman, I. Pinkas, S. G. Wolf, B. Rybtchinski, *J. Am. Chem. Soc.* **2008**, *130*, 14966–14967.

[8] a) F. Würthner, *Chem. Commun.* **2004**, 1564–1579; b) M. Kazmaier, R. Hoffmann, *J. Am. Chem. Soc.* **1994**, *116*, 9684–9691.

[9] C. Shahar, J. Baram, Y. Tidhar, H. Weissman, S. R. Cohen, I. Pinkas, B. Rybtchinski, *ACS Nano* **2013**, *7*, 3547–3556.

[10] a) A. Chaudhary, R. Patra, S. P. Rath, *Indian J. Chem. Sect. A* **2011**, *50*, 1436–1442; b) E. Shirman, A. Ustinov, N. Ben-Shitrit, H. Weissman, M. A. Iron, R. Cohen, B. Rybtchinski, *J. Phys. Chem. B* **2008**, *112*, 8855–8858.

[11] T. M. Wilson, T. A. Zeidan, M. Hariharan, F. D. Lewis, M. R. Wasielewski, *Angew. Chem.* **2010**, *122*, 2435–2438; *Angew. Chem. Int. Ed.* **2010**, *49*, 2385–2388.

[12] H. Marciniak, X. Q. Li, F. Würthner, S. Lochbrunner, *J. Phys. Chem. A* **2011**, *115*, 648–654.

